Influence of generation number on the dewetting of hypergraft poly(2-ethyl-2-oxazoline) films

Kathleen A Barnes, Jack F Douglas,* Da-Wei Liu, Barry Bauer, Eric J Amis
and Alamgir Karim*

Polymers Division, National Institute of Standards and Technology, Gaithersburg, MD 20899, USA

Abstract: We investigate the influence of polymer branching (generation number *G*) on the dewetting of hypergraft poly(2-ethyl-2-oxazoline) (PEOX) polymer films from model non-polar synthetic polymer and inorganic substrates. The present study contrasts the cases of a zeroth generation *G*0 hypergraft, which is a comb polymer, and a *G*2 hypergraft, which resembles a nearly spherical 'microgel' particle. The early stage of dewetting is found to be similar in the *G*0 and *G*2 films and is largely independent of substrate (entangled polystyrene film or acid-cleaned silica wafer). However, the late stage of dewetting in the *G*2 films differs significantly from the *G*0 films because of an inhibition of hole coalescence in the intermediate stage of film dewetting. The holes in the *G*2 hyperbranched films continue to grow in size until they impinge on each other to form a foam-like structure with a uniform 'cell' size. The boundaries of these cells break up and the vertices of the former cellular network retract to form a relatively *uniform* droplet configuration. In contrast, hole coalescence in the *G*0 films occurs readily, leading to a polydisperse hole size distribution, and the fluid borders of the holes break up to form the non-uniform 'Voronoi' droplet configuration normally associated with film dewetting. Similar trends have been observed in the dewetting of linear polymer films where entangled polymers behave similarly to the branched (*G*2) polymers of the present study. This effect is attributed to the viscoelasticity of the *G*2 hyperbranched polymer fluid.
© 2000 Society of Chemical Industry

Keywords: dewetting; hypercraft polymer; film; foam

1. INTRODUCTION

The dewetting of polymer films from organic and inorganic substrates is a ubiquitous phenomenon arising in numerous coatings and biotechnology applications.[1–3] The morphology of the film in the late stage of dewetting is dependent on both the type of polymer and substrate.[4–6] Relatively few studies have focused on factors affecting the morphology and kinetics of dewetting in the intermediate and late stages where the morphology is dominated by hole coarsening (coalescence together with diffusive growth) and the break up of the film into droplets.[7] In the present paper, we focus on the late stage of dewetting to identify factors relevant for controlling the final morphology of dewetted polymer films.[8]

It is well known that polymer entanglements can have a large influence on the 'stability' of polymer films. Often it is only possible to form polymer films on inorganic substrates over long times if the polymers are 'entangled' or locked into a non-equilibrium 'glassy' state. For example, it has recently been shown that the sulfonation of polystyrene greatly suppresses film dewetting on silica substrates, and it was suggested that this film stabilization might be a consequence of

chain 'entanglement' arising from sulfonation.[9] This type of film stabilization is only a kinetic rather than an equilibrium 'stabilization' effect, so that dewetting is not inhibited indefinitely. Moreover, because the dewetting process depends critically on the film-rupture process associated with hole coalescence, we can anticipate significant changes in the film morphology arising from the non-Newtonian fluid properties of the dewetting polymer. There have been recent studies contrasting dewetting of polymer films on inorganic and viscous polymer substrates[10] so we also examine the role of substrate type on film dewetting.

In the present paper, we contrast the dewetting process in model polymer films from model non-polar synthethic polymer and inorganic substrates. The dewetting films are chosen to be generation *G*0 and *G*2 hypergraft polyethyloxazoline (PEOX) because the viscoelastic properties of PS hypergraft polymers having a similar topology have previously been shown to have significant changes in their viscoelasic properties with generation number *G*.[11] The *G*0 hypergraft PS polymers have properties similar to unentangled linear or lightly branched (combs, few-arm stars) polymers, while the *G*3 PS hypergraft formed a gel-like

---

material at room temperature.[11] The *G*2 PS hypergraft remains a liquid and has an extended plateau in its shear stress relaxation that is reminiscent[11] of entangled linear polymers[12] or micro-gel particles.[13] Thus, the *G*2 PEOX hyperbranched polymers of the present study can be expected to exhibit the flow properties of a highly viscoelastic fluid, and below we compare the dewetting properties of the *G*2 fluid to modestly entangled linear polymer fluids. The substrates were a highly viscous polymer layer (entangled PS) that did not dewet from its silica underlayer on the timescales of our measurements and the hyperbranched polymers were also spun-cast directly onto acid-cleaned silica wafers. Significant changes in the dewetting patterns were observed because of the generation number of the hypergraft, while the substrate type was observed to have a lesser influence on the late-stage dewetted film morphology. The change of the dewetting patterns is attributed to a change in the hypergraft polymer film viscoelasticity with *G*.

2. EXPERIMENTAL

Thin films of deuterated PS [poly(styrene-d_8)] with a reported mass M_w of 188 000 g mol^{-1} and polydispersity M_w/M_n of 1.05 (According to ISO 31-8, the term molecular weight has been replaced by 'relative molecular mass' M_r. The older, more conventional, notation for number-average (M_n) and weight-average (M_w) molecular weights is utilized in the present paper.) were obtained from Polymer Laboratories (Certain commercial equipment, instruments, and materials are identified in this paper in order to adequately specify experimental procedure. Such identification does not imply recommendation or endorsement by NIST, nor does it imply that the materials or equipment identified are necessarily the best available for the purpose.) were spun cast from toluene solutions at a polymer mass fraction of 1% at 1000 revolutions per minute (rpm) onto acid-cleaned silica substrates and annealed under vacuum at 130 °C for 30 min to remove any residual solvent in the film. The entanglement molecular mass M_e of PS is 1.8×10^4 g mol^{-1} (ref 15) so that the substrate polymer films are highly entangled. The silica wafer substrates were previously cleaned in a solution with 70% volume fraction concentrated sulfuric acid and 30% volume fraction hydrogen peroxide at 80 °C for 1 h, followed by rinsing in deionized water and drying under nitrogen gas.

Hypergraft and linear poly(2-ethyl-2-oxazoline) (PEOX) solutions (generations *G*0 and *G*2, respectively[16] having a 1% mass fraction in methanol were spun cast at 2000 rpm onto the PS-coated silica or onto bare acid-cleaned silica substrates. The films were then imaged as cast after annealing under vacuum for various time intervals. Reflection optical microscopy images were taken using a Nikon microscope. The PEOX hypergraft polymers (sometimes

termed 'dendrigraft' polymers) were obtained from Michigan Molecular Institute and their synthesis was previously reported.[16] The samples studied were a linear PEOX polymer with M_w 30 000 g mol^{-1} and dendrigrafts in the series [100$_x$–100] with $x = 1$ and 3, where 100 denotes the degree of polymerization of backbone and the grafts.[16] The x designation refers to *G*1 in the present work. Properties of topologically similar PS hypergraft polymers for generations 0, 1, 2 and 3 have recently been described by Gauthier and coworkers,[17] and PS hyperbranched molecules in monomolecular films have been directly imaged by atomic force microscopy.[18] We expect the PEOX hypergraft molecules to have a similar structure to the PS hypergrafts. Characterization of the PEOX hybergraft polymers is described by Yin *et al.* [16]

3. RESULTS

The dewetting of linear polymers of low molecular weight ('unentangled') films of moderate thickness ($10 < L < 100$ nm) has been intensively investigated and a common pattern of dewetting has been established.[4–6] Holes form by nucleation (heterogeneous nucleation from impurities and homogeneous nucleation from surface undulations) at random positions at the film boundary, and these circular holes grow slowly in the early stage of dewetting. At a later stage of dewetting there is strong tendency for the holes to coalesce, and this coalescence process largely determines the nature of the late-stage dewetting pattern. Liquid thread-like borders of the 'cells' of dewetted surface break up by a capillary wave instability to leave a constellation of droplets distributed in the form of a Voronoi-like pattern.[4,5]
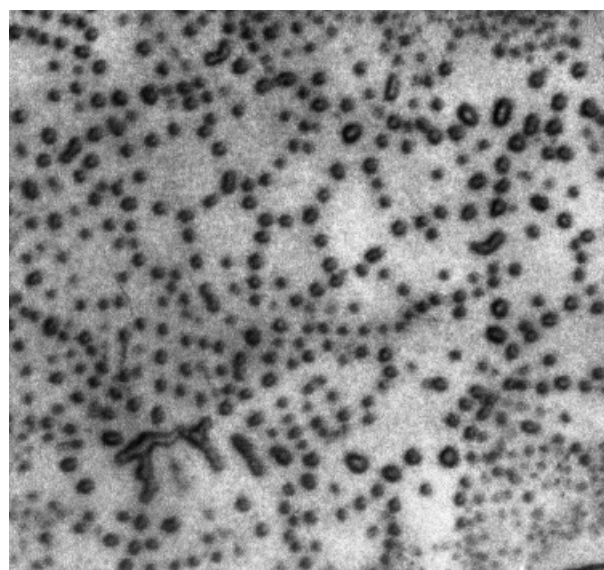

Figure 1. Late-stage dewetting of a *G*0 PEOX film on a PS substrate at 135 °C after 25 min. Thickness of PEOX and PS layers are estimated to be in the range ×20–50 nm and ×50–100 nm, respectively. Image width is 125 μm. This dewetting pattern resembles observations of late-stage dewetting in unentangled linear polymer films.

Figure 1 shows the dewetting for a *G*0 PEOX film at a late stage of dewetting ($t = 25$ min, $T = 135\,°C$) from a viscous polystyrene substrate. This dewetting morphology is typical of previous studies[4,5] of low molecular weight ('unentangled') polymer films dewetting for this range of film thickness, so we do not discuss this case further. This 'normal' dewetting scenario should be kept in mind when we compare the dewetting of highly branched (*G*2) polymer films from the same substrate.

The as-cast film *G*2 PEOX film is smooth, and circular holes form at random positions within the plane of the film. (Image not shown because of the similarity to many previously published images of early stage film dewetting.)[4,5] The initial stage of the dewetting process is then remarkably similar to the observations on unentangled linear and *G*0 films.[4,5] However, as the holes of the entangled polymer films grow to sufficient size to impinge on each other, we see a striking change in the dewetting dynamics. In the *G*2 polymer film, the holes press against each other, but do not seem to coalesce. Similar behaviour has been observed in entangled linear-chain polymer films in which the molecular weight is not so high as to prevent dewetting.[10] In Figs 2 and 3 we see direct evidence for the hole growth in time and the tendency for the holes to become distorted as they press against each other during growth (note the clover-leaf-like shapes in Fig 3). The shape distortions are similar to those found in (mathematical) two-dimensional soap bubbles where the distortions arise to minimize the surface perimeter, subject to constraints against coalescence.[19–21] These

Figure 3. Intermediate-stage dewetting of a *G*2 PEOX film in the 'hole-distortion' regime. Film shown corresponds to an annealing time of 15 min at 130 °C. The holes continue to grow in size and impinge on each other, leading to hole shape distortion. Similar distortions of boundary shapes are seen in interacting soap bubbles.[28,29] Image width is 90 μm.

observations suggest that the highly branched (*G*2) hypergraft PEOX films have a relatively large surface viscosity[22] that inhibits hole coalescence. A similar inhibited coalescence is observed in the phase separation of reactive blends of polycarbonate and poly(methyl methacrylate) where a polymer layer reactively forms the interface of the phase separating blend components.[23] Inhibited coalescence is also observed in the phase separation of entangled poly(vinyl methyl ether) (PVME) in water, where droplet coalescence is almost entirely suppressed.[24] The exact nature of this surface viscoelasticity remains to be quantified, but it seems clear that non-trivial surface viscoelaetic effects exist in certain high molecular weight polymer fluids. Interestingly, the present observations on *G*2 hypergraft PEOX suggest that these polymers might have similar viscoelasic properties to entangled polymer fluids.

Antonietti *et al*[13,14] have recently pointed out that highly branched and nearly spherical nanogel particles can exhibit bulk viscoelastic properties remarkably similar to melts of entangled linear polymers, and Hempenius *et al*[11] have noted a great similarity of the viscoelastic spectra of *G*2 hypergraft PS polymers to the 'microgel' particles of Antonietti *et al*.[13,14] Moreover, Gauthier *et al*[25] have recently observed a tendency of *G*2 PS hypergraft molecules to form pearl-like chains of hypergraft molecules when Langmuir films of the dendrigraft polymer are spread onto
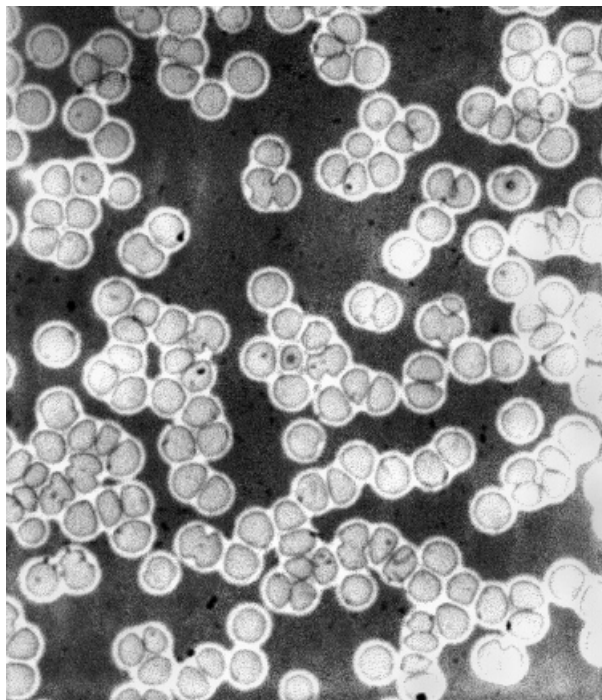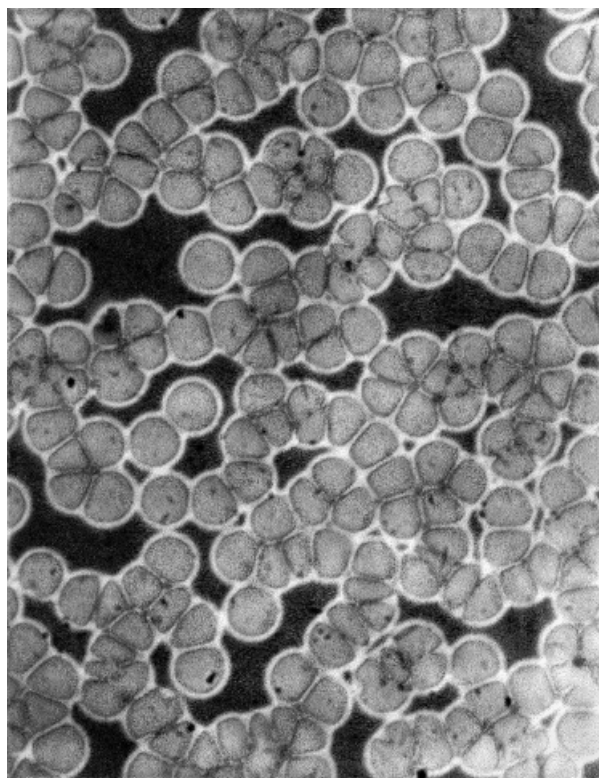

Figure 2. Intermediate-stage dewetting of a G2 PEOX film in the 'hole-chaining' regime. Film shown corresponds to an annealing time of 10 min at 130 °C. Note the tendency of the holes formed in the early stage of dewetting (early stage not shown) to 'chain' and the inhibition against hole coalescence. Image width is 90 μm.

water. This type of clustering is suggestive of living polymerization type particle aggregation[26] in these highly branched polymers, and this aggregation phenomenon could explain the viscoelasic properties of these branched-molecule fluids.[27] (Douglas and Habbard[27] have suggested a living polymerization model of chain entanglement based on the idea that collective chain motion in the form of equilibrium clusters occurs when the average chain dimensions become sufficiently large in comparison to their average chain cross-sectional diameter. An Onsager-type condition for interparticle correlation then governs the 'entanglement' interaction in this model. Temperature is usually the control parameter for living polymerization, so that temperature studies of the rheological properties of hyperbranched polymer fluids should be especially interesting. Thermally reversible gel transitions can be expected either upon heating or cooling in these systems, depending on the polymer and solvent chemistry.[26])

At a still later stage of the PEOX dendrigraft film dewetting, the borders of the hole clusters begin to percolate and form a cellular network structure. Figure 4 shows some of these cells as their boundaries begin to break up into droplets by capillary instability. This signals the final droplet stage ($t = 120\,min$) of dewetting, and the resulting droplet configuration for this film is shown in Fig 5. The film morphology seems to

Figure 5. Late-stage dewetting of a G2 PEOX film in the droplet regime. Film shown corresponds to an annealing time of 120 min at 130 °C. Fluid cell borders shown in Fig 4 break up into droplets. Note relative uniformity of droplet size and coverage in comparison to the G0 film shown in Fig 1. The break-up of the fluid cell borders is accompanied by a retraction of the liquid into droplets that lie near the cell vertices of the former hole 'froth'. The droplet distribution does not appear to evolve significantly in this late stage of dewetting, apart from a tendency for the droplets to become increasingly circular. Image width is 90 μm.
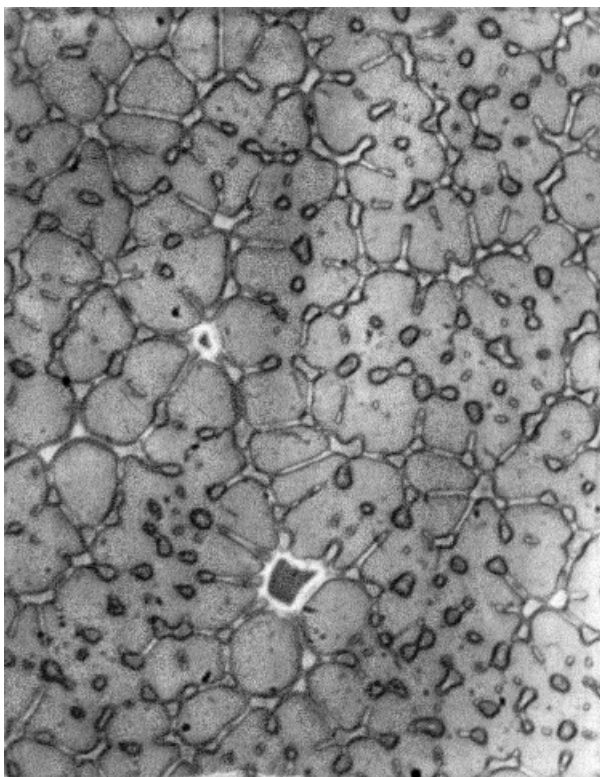

Figure 4. Intermediate-stage dewetting of a G2 PEOX film in the 'froth' regime. Film shown corresponds to an annealing time of 45 min at 130 °C. The connectivity of the hole clusters spans the entire systems, forming a foam-like network ('froth'). Observe the relative uniformity of the cell size and shape and the widths of the fluid borders of the cells. Image width is
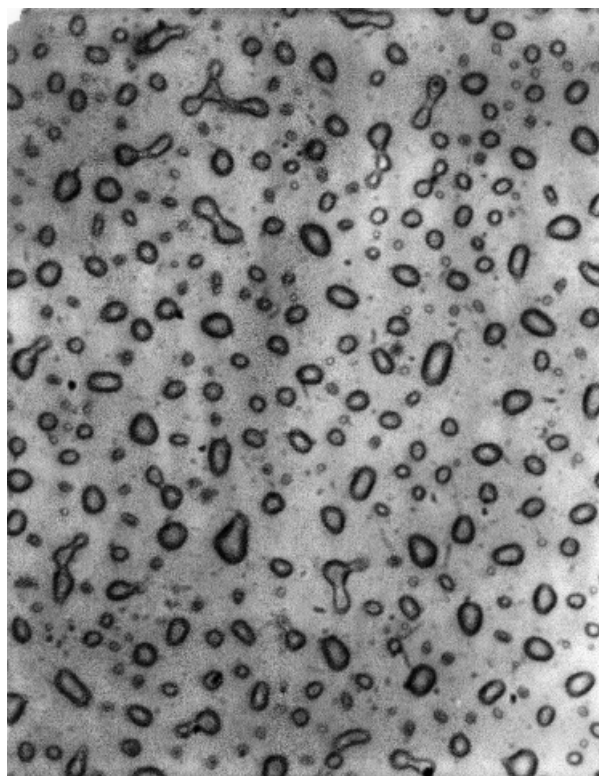
remain in the form of Fig 5 upon further annealing, and no significant change in the shape or size of the droplets is seen even after a time $t = 300\,min$. Note the relative uniformity of the droplet configuration and droplet sizes in comparison to Fig 1. Film viscoelasticity appears to have a large impact on the final morphology of the dewetted film. A similar effect is found for a solid inorganic substrate.

In Fig 6 we show the image of dewetting of G2 PEOX film from an acid-cleaned silica wafer. This late-stage film dewetting pattern should be compared to the one found for the polystyrene substrate in Fig 5. A cellular dewetting pattern with cells having uniform size has been observed for high molecular polystyrene films dewetting from silanized silica wafer,[4,5] and these uniform cellular patterns are the precursors of relatively uniform droplet arrays (see Fig 4). The droplet configuration in Fig 6 is quite uniform in comparison to dewetting patterns found for the G0 film. Figure 7 shows the late-stage dewetting pattern of the G0 PEOX from the silica wafer as a control measurement. The dewetting pattern of the G0 film corresponds to conventional observations for late-stage dewetting. (Essentially the same results were also obtained for a linear chain PEOX film of molecular
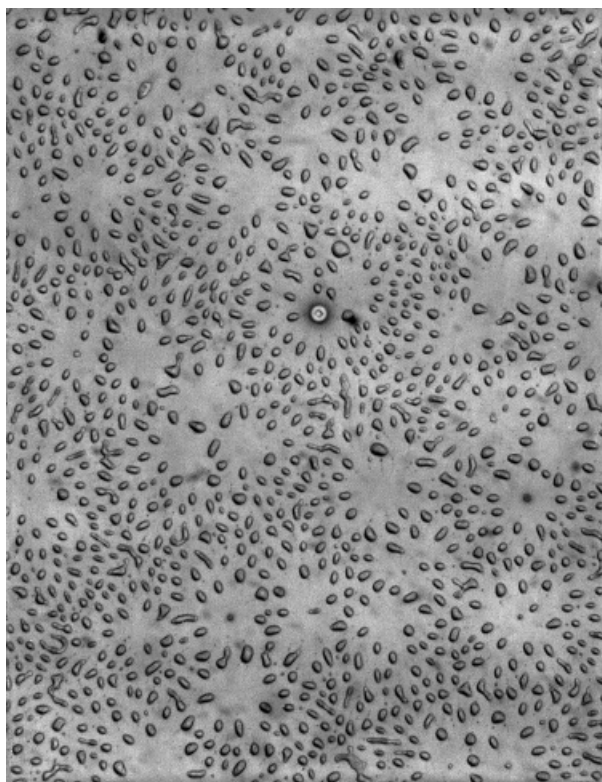
Figure 6. Late-stage dewetting of a *G*2 PEOX film dewetting from an acid-cleaned silica substrate. Film was annealed at 120 °C for 120 min. As in the case of the films on PS substrates, the *G*2 polymer films on acid-cleaned silica substrates form a relatively uniform distribution of droplets. However, note the presence of a large-scale correlation in the droplet dewetting patterns that we have informally termed 'floral' patterns. We suspect that these 'floral' patterns arise from a superposition of two distinct dewetting processes. Surface heterogeneities can rapidly nucleate circular dewetted

altered in our studies of highly branched (*G*2) PEOX and lightly branched (*G*0) polymer dewetting from PS and acid-cleaned silica substrates, and we suspect a similar origin in terms of the fluid viscoelasticity. The frustration of the normal hole coalescence process leads first to a clustering of holes, then their deformation as the holes grow and impinge on each other. Finally, the holes form a network of dewetting cells having a rather uniform cell size. The fluid walls of these cells break up by a capillary instability, leading to uniform droplet configurations. In the absence of entanglement, hole coalescence leads to a hierarchical hole size distribution and a broad distribution of droplet sizes. The present results suggest that film viscoelasticity has a qualitative effect on the final morphology of dewetted polymer films. The nature of the substrate (viscous polymer film or silica wafer) seems to have a lesser effect on the dewetting morphology in our measurements. In view of these observations, it is important to make further characxterizations of the viscoelasticity of highly branched hypergraft molecules such as PEOX and other molecules exhibiting highly viscoelastic or 'entanglement' flow behaviour. Further measurements are also needed on entangled linear polymer films to establish better the influence of their viscoelasticity on dewetting. These measurements are needed for more quantitative comparisons between the phenomenology
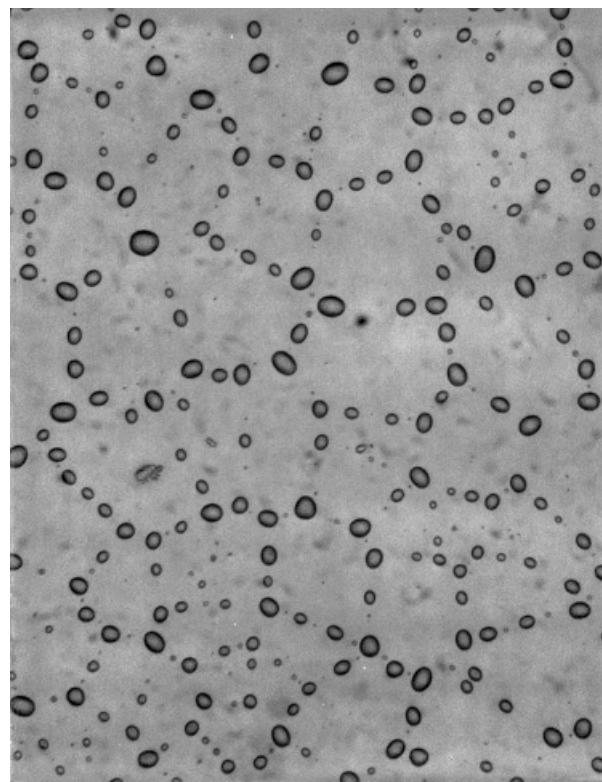
weight $M_w = 30\,000\,\mathrm{g\,mol^{-1}}$ and these results are not shown because of their similarity to the *G*0 films.) Thus, polymer branching (and presumably the associated change in film viscoelasticity) can have a significant influence on the dewetting morphology, while the nature of the substrate (organic or inorganic) has a weaker effect on dewetting in our measurements. Changes in the rate of dewetting arising from the substrate chemistry can generally be anticipated however, because the driving force for dewetting depends on the surface energy.

4. DISCUSSION

Polymer entanglement is known to have an impact on the stability of thin films against dewetting, although little quantitative study of the effect of viscoelasticity on film dewetting exists. The suppression of dewetting due to entanglement is predominantly a kinetic effect, but the non-Newtonian nature of high molecular weight linear polymer films can also affect the *qualitative* late-stage dewetted film morphology. Thus, the poorly understood chain 'entanglement' effect in linear polymers involves more than a purely kinetic effect on dewetting. Similarly, the dynamics of the hole rupture process during film dewetting is significantly

Figure 7. Late-stage dewetting of a *G*0 PEOX film dewetting from an acid-cleaned silica substrate. Film was annealed at 120 °C for 120 min. As in Fig 1, a 'Voronoi tessalation' pattern is found, reflecting the break-up of the hierarchical network structure formed through facile hole coalescence.[28] Image width is 300 μm.

of dewetting in entangled linear high and hyper-branched polymer films.

We make some final remarks about the theoretical modeling of the intermediate stage dewetting morphology. A hole in a thin polymer film can be considered a 'bubble' in an idealized two-dimensional liquid, and cellular patterns formed at high hole area fraction concentrations can be expected to be very similar to the patterns observed in idealized two-dimensional soap bubble froths. There is indeed a striking resemblance between the cellular structures observed in our measurements on $G0$ and $G2$ dewetting films, the dewetting patterns of unentangled and entangled polymer films of linear polymers, and near two-dimensional soap 'froths'.[28,29] Moreover, similar patterns are also observed in other thin films[29] (magnetic bubbles and lipid monolayer bubbles; see Figs 1 and 2 of ref. 28). In some nearly two-dimensional 'froths', where the bubbles are stable against rupture, the froth evolves into a cellular pattern with regular sized cells, similar to our dewetting polymer films in intermediate-stage dewetting. The easy coalescence of the bubbles drives the froth into 'scaling state' in which a broad cell size distribution exists. The average scale of the froth pattern grows in time, much like coarsening during fluid phase separation. This unstable froth structure resembles the entangled polymer film morphology in the intermediate stage of dewetting. Magnasco[28] has sought to characterize the factors governing these two conspicuously different types of froth evolution patterns, and this analogy between two-dimensional froths and dewetting films should be helpful in quantifying the geometry of dewetting patterns and understanding the general patterns of film dewetting expected in thin polymer films. The structure of two-dimensional froths is governed by geometrical constraints (eg, Euler relations between number of froth vertices, faces and edges) and the dynamics of the cell coarsening. It would be interesting if this rich foam phenomenology also describes film dewetting.

REFERENCES
1 Wu S, *Polymer Interface and Adhesion*, Marcel Dekker, New York (1982).
2 Licari JJ and Hughes LA, *Handbook of Polymer Coatings for Electronics: Chemistry, Technology and Applications*, Noyes Publications, New Jersey (1990).
3 Service RF, *Science* **278**:383 (1997).
4 Reiter G, *Phys Rev Lett* **68**:75 (1992).
5 Reiter G, *Langmuir* **9**:1344 (1993).
6 Stange TG and Evans DF, *Langmuir* **13**:449 (1997).
7 Xie R, Karim A, Douglas JF, Han CC and Weiss RA, *Phys Rev Lett* **81**:1251(1998).
8 Sharma A and Khanna R, *Phys Rev Lett* **81**:3463 (1998).
9 Feng Y, Karim A, Weiss RA, Douglas JF and Han CC, *Macromolecules* **31**:484(1998).
10 Faldi A, Composto RJ and Winey KI, *Langmuir* **11**:4855 (1995).
11 Hempenius MA, Zoetelief WF, Gauthier M and Möller M, *Macromolecules* **31**:2299 (1998).
12 Ferry JD, *Viscoelastic Properties of Polymers*, Wiley, New York (1980).
13 Antonietti M, Bremsler W and Schmidt M, *Macromolecules* **23**:3796 (1990).
14 Antonietti M, Pakula T and Bremser W, *Macromolecules* **28**:4227 (1995).
15 Roovers J and Graessley WW, *Macromolecules* **14**:766 (1981).
16 Yin R, Tomalia DA, Kukowska-Latallo J and Baker JR, *PMSE Prepr* **71**:206(1997).
17 Frank RS, Merkle G and Gauthier M, *Macromolecules* **30**:5397 (1997).
18 Sheiko SS, Gauthier M and Möller M, *Macromolecules* **30**:2350 (1997).
19 Foisy J, Alfaro M, Brock J, Hodges N and Zimba Z, *Pacific J Math* **159**:47 (1993).
20 Morgan F, *Pacific J Math* **165**:347 (1994).
21 Almgren Jr, FJ and Taylor JF, *Sci Am* **235**:82 (1976).
22 Wasan DT, McNamara JJ, Shah SM and Sampath K, *J Rheol* **23**:181 (1979).
23 Karim A, Douglas JF, Satija SK, Goyette RJ and Han CC, *Macromolecules* **32**:1119 (1999).
24 Tanaka H, *Macromolecules* **25**:6377 (1992).
25 Gauthier M, Cao L, Rafailovitch MH and Sokolov J, *Polym Prepr* **40**:114(1999).
26 Dudowicz J, Freed KF and Douglas JF, *J Chem Phys* **111**:7116 (1999).
27 Douglas and Hubbard , *Macromolecules* **24**:3163 (1991).
28 Magnasco MO, *Philos Mag B* **65**:895 (1992).
29 Weaire D and Rivier N, *Contemp Phys* **25**:59 (1984).